JOURNAL OF MATERIALS SCIENCE 29 (1994) 33–38

Fibre–matrix interfacial failure sequences in translaminar flexure of glass–epoxy composites

K. PADMANABHAN, KISHORE
Centre for Advanced Studies, Department of Metallurgy, Indian Institute of Science, Bangalore 560 012, India

A detailed fractographic analysis is reported for the fibre–matrix interfacial failure sequences in the translaminar flexure testing of glass–epoxy composites of two different resin formulations. The influence of curing conditions, loading rates and voids on the mechanical data obtained is discussed. The fracture mechanisms are explained on the basis of the shear couple concept.

1. Introduction

Most of the composite materials reinforced with continuous fibres exhibit non-linear stress-strain behaviour in at least one of the principal directions. The degree of non-linearity varies from composite to composite and is mainly due to the non-linear stress–strain behaviour of the matrix material which greatly affects the transverse modulus and shear modulus of the composite. While the effect of this non-linearity of the matrix material on the tensile properties is negligible, the same is not found in the flexural and interlaminar shear properties.

The three-point flexure test, used to determine flexural strength and modulus, is one of the most common and also one of the most misunderstood tests for composites [1]. This test specifies procedures which provide reliable data on strength, but as shown by many [1–4], the modulus values can be misleading because of shear. The flexural properties are thus laminate properties rather than just material properties. To be precise, the flexural properties for the interlaminar or translaminar configuration [4] are governed by the alignment or misalignment of the fibre layers or fabric layers. Many researchers have investigated the interlaminar flexural properties and fracture behaviour of laminated continuous fibre-reinforced composites. However, when it comes to flexural properties and fracture behaviour in the translaminar configuration, only a few reports are available. Fischer *et al.* [5] and Gershon and Marom [4] have made some interesting contributions towards these aspects of mechanical behaviour. Padmanabhan and Kishore [6] have studied the role of alumina particulate additions on the interlaminar and translaminar flexure of glass–epoxy composites.

The purpose of this work was hence to look into the fracture behaviour of laminated glass–epoxy composites in the translaminar testing configuration and carry out a rudimentary microscopic analysis into the cause of fracture. The time dependence of the flexural fracture properties was also investigated for two glass–epoxy composites with different epoxy formulations and the observed non-linear characteristics were explained. Different samples were tested to various stages in the post-fracture region and their fracture surfaces were carefully scanned and analysed to obtain an insight into the exact nature of the sequences leading to the failure of the composites.

2. Experimental procedure

The reinforcing material used was an E-glass fabric of 7 mil (178 μm) plain weave, having a density of 2.54 g cm^{-3} with an epoxy-compatible silane finish. The epoxy resin used was Hindustan Ciba-Geigy Araldite LY 556 with a room-temperature curing hardener HY 951 (formulation I) in one case and a high-temperature curing hardener HY 972 (formulation II) in the other case.

A hand lay-up was initially done which was followed by compression in a hydraulic press. While for formulation I the curing was carried out at room temperature, for the other the curing temperature was 120 °C. Thus glass–epoxy laminates with dimensions of 300 mm × 300 mm × 5 mm were fabricated with two different formulations of epoxy resin. To assess the volume fraction of the fibres in the laminates, the standard burn-out test was conducted. From the different weighings, the volume fractions of the fibres were estimated as 0.57 for the composite with resin formulation I and 0.59 for the composite with formulation II.

The extent of cure of the resin formulations was determined by differential scanning calorimetry, (DSC) using a Perkin Elmer DSC II thermal analyser at a heating rate of 10 ° min^{-1}.

Translaminar test specimens of dimension 100 mm × 5 mm × 5 mm [6] were carefully machined from the laminates. In these specimens the breadth and the depth were kept equal in order to prevent buckling during bending [6, 7]. These tests were carried out in an Instron 8032 machine, at a support span to depth ratio of 16 to 1 [8]. The mid-span roller and the two support rollers were of 25 mm diameter, which reduced local stress concentrations due to the roller

0022–2461

while the specimens underwent the tests. Three different crosshead velocities of 0.0035, 0.035 [8] and 0.35 mm s^{-1} were used to study the effect of loading rate on flexural properties like the modulus of elasticity in bending (E_B) and the maximum fibre stress (MFS). In selected samples the tests were stopped at various stages prior to the total failure of the specimen, as indicated in Fig. 1. This was done with the objective of carrying out a detailed microscopic analysis of such stages and hence the failure sequences. Partially as well as completely fractured specimens were carefully sectioned and then sputter-coated with a thin layer of gold–palladium alloy and their fracture features were observed in a scanning electron microscope (SEM) in the secondary electron mode. The area of cross-section in the failed specimens chosen for scanning is shown in Fig. 2. The tensile face and the compressive face of the completely failed samples were not considered for fractographic analysis due to the following reasons.

1. Significant fibre pull-out of the axial fibres along the length of the sample renders observation of the transverse fibre–matrix interface very difficult.
2. The compression region shows buckling of the transverse fibres and extensive post-fracture damage which lead to distortion of fracture surface details due to the debris settling on the above-mentioned region.

Added to the points mentioned above, it must be noted that the area selected for fractographic analysis of the failure sequences exhibits shear deformation along the length as well as the depth of the samples. The shear component of the total deflection in the sample becomes appreciable when the span to depth ratio is 16/1 [1].

3. Results and discussion

3.1. Thermal analysis

Fig. 3 shows the DSC thermograms of the two composites with different resin formulations. Specimens cut from the two differently cured laminates were dynamically scanned at a rate of 10 °C min^{-1} in the range 300–450 K, to assess whether a good degree of cure was obtained earlier in the laminates or not. Curing appears as an exothermic reaction on the DSC trace and the area under this peak is a measure of the degree of cure. Here, no exotherms were observed on the specimens cured with the resin formulation I as well as II, indicating completion of cure.

3.2. Flexural properties

Fig. 4 shows the relationship between the modulus of elasticity in bending (E_B) and strain at three different crosshead velocities, for the two different composites. These isochronous curves [9] exhibit a greater degree of non-linearity in the glass–epoxy composite with resin formulation II, added to the fact that the E_B

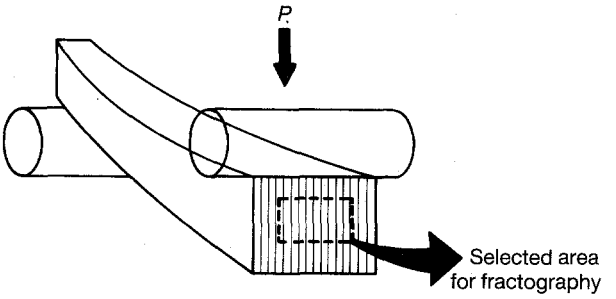

Figure 2 Translaminar flexure test showing the area selected for fractography.

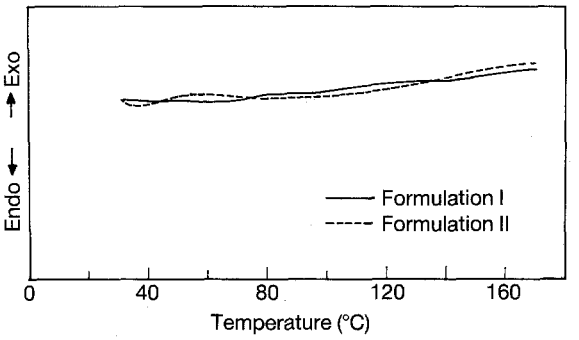

Figure 3 DSC thermogram of the two composites with resin formulations (—) I and (– – –) II, in dynamic scanning at a heating rate of 10 °C min^{-1}.

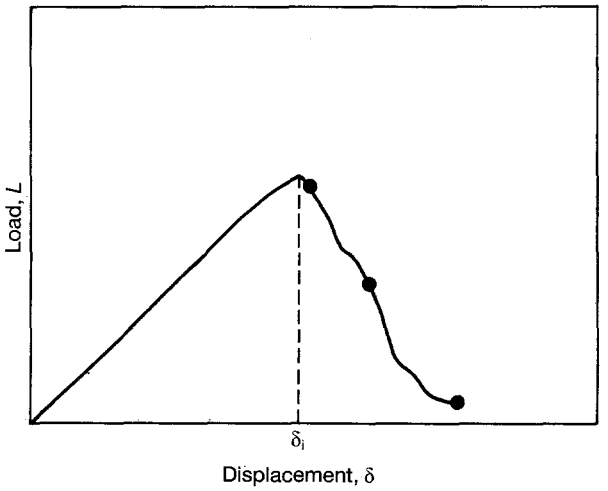

Figure 1 Schematic load–deflection diagram showing (●) the various stages at which the tests were stopped.

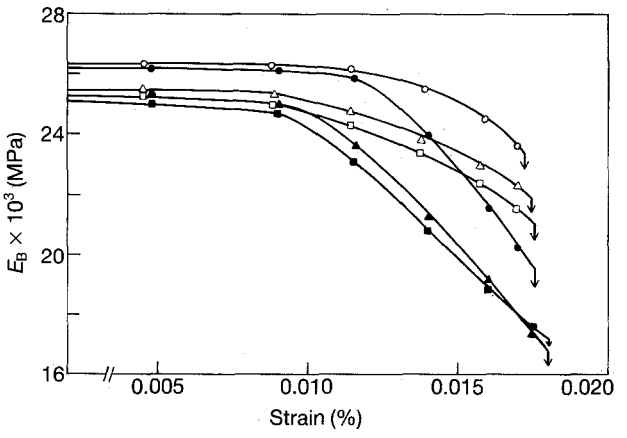

Figure 4 Isochronous curves of modulus of elasticity in bending against strain, for the two composites at three different crosshead velocities. Formulation I : (□) 0.0035, (△) 0.035, (○) 0.35 mm s^{-1}. Formulation II : (■) 0.0035, (▲) 0.035, (●) 0.35 mm s^{-1}.

values are also less when compared to the composite with resin formulation I. Table I shows the MFS values of the two composites at three loading rates. The marginal loading-rate sensitivity exhibited by both the composites, though consistent, does not seem to depend appreciably on the formulation of the resin.

The E_B values recorded for the two different composites are well below the rule-of-mixtures (ROM) values for their stipulated volume fractions (approximately 40 000 MPa is the ROM value for $V_f = 0.58$) [4]. This is in agreement with the inference that the ROM assumed a void-free and defect-free composite and only sets an upper bound to the axial E_B value. Tsai [10] modified the ROM expression as $E_c = k(E_f V_f + E_m V_m)$ where E_f, E_m are the moduli of the fibre and matrix, respectively; $V_f + V_m = 1$ and E_c is the composite modulus. The factor k accounts for different states of fibre misalignment existing in the translaminar testing configuration. At this stage it is worth noting that previous investigators [11] have pointed out that the water-boil treatment does not influence the modulus values of a composite. Thus, the reason for the discrepancy in the E_B values of the two composites could be related to the degree of misalignment of the fibres in the two composites. SEM observations show that void formation between the fibre layers due to curing, is more when the high-temperature resin (formulation II) is used (Fig. 5). The presence of such voids leads to increased misalignment of fibre layers during the translaminar bend test, thus reducing their E_B values.

The MFS values show a marginal loading-rate sensitivity for the three loading rates. As fibre misalignment can be shown to cause variations in the E_B values, the pinning and blunting mechanisms can be invoked to explain the variations in the MFS values of a translaminar flexure specimen. Our earlier work [6] has shown that continuous crack-front propagation at higher loading rates leads to an increased degree of crack-tip pinning, bowing-out phenomena and crack-tip blunting. Here, in the composites with formulation II resin, the increased occurrence of blunting events for higher loading rates at the voids, which normally delays the ultimate fracture, is offset by the increased misalignment of fibres due to the presence of the voids themselves. This seems to explain why the two composites do not show any appreciable difference in their loading-rate sensitivity.

TABLE I Maximum fibre stress of the two composites at three different crosshead velocities

	MFS (MPa)		
	0.0035 mm s^{-1}	0.035 mm s^{-1}	0.35 mm s^{-1}
Formulation I	386	401	415
Formulation II	378	392	407

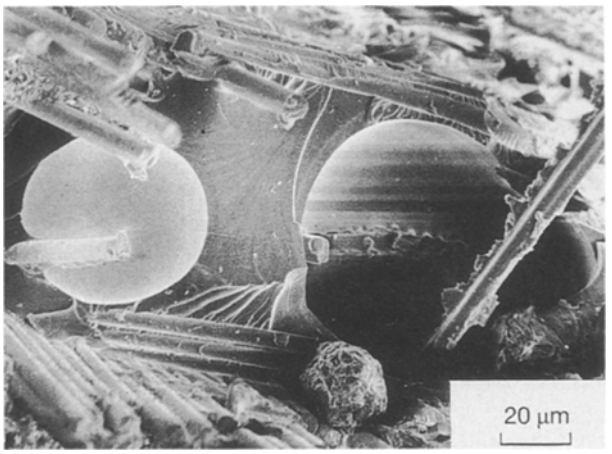

Figure 5 Voids formed during curing in the composite with formulation II resin.

3.3. Fracture mechanisms

Some of the general translaminar fracture features observed by previous investigators are extensive fibre pull-out, fibre matrix debonding, fibre breakage and matrix stretching in the tensile side, and microbuckling of fibres, chop marks on fibre tips and debris formation on the compressive side. Practically no reports are available regarding the fracture features obtained in a sequential way. Especially in woven fabric composites, a detailed study of sequential failure events in the axial and transverse fibre–matrix interfacial regions seems unavailable from our perusal of literature.

Fractographic analysis, carried out mainly to understand the failure sequences of the two composites in the translaminar testing condition, revealed many interesting features at the fibre–matrix interface. The fracture regions classified as resin-rich and fibre-rich regions show set patterns in the failure sequences at the interface. The general pattern of failure involves the following steps:

1. Shear cracks are formed at an angle to the interface, in the region selected for fractography.
2. As the shear deformation proceeds at the fibre–matrix interface of transverse fibres situated along the loading direction, an unbalanced shear couple is formed which promotes the occurrence of secondary cracks in resin-rich regions, starting from the shear cracks described above (Fig. 6b). With further deformation, the region near the interface formed by the branching of cracks separates along with the fibre from the matrix, to produce a cusp-like appearance.

In fibre-rich regions (Fig. 7) hackles and scallops between two fibres situated in the transverse direction are a common occurrence. Towards the tensile face, fibres oriented parallel to the direction of crack propagation tend to form orthogonal-shaped hackles in the matrix [12]. Otherwise, an unbalanced shear couple causes the hackles to be formed at an angle to the fibres. The shear deformation of the fibre–matrix interface situated along the loading direction is illustrated in Fig. 7a–c. The hackles thus formed angle out more due to the non-linear shear deformation, and after the separation of the fibre and matrix can be seen as miniscule cusps along the fibre surfaces.

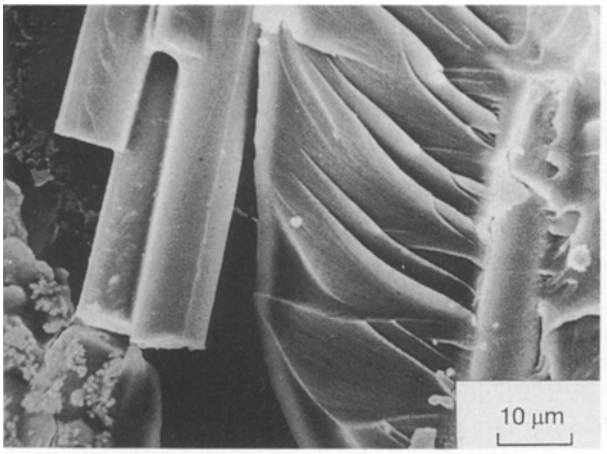

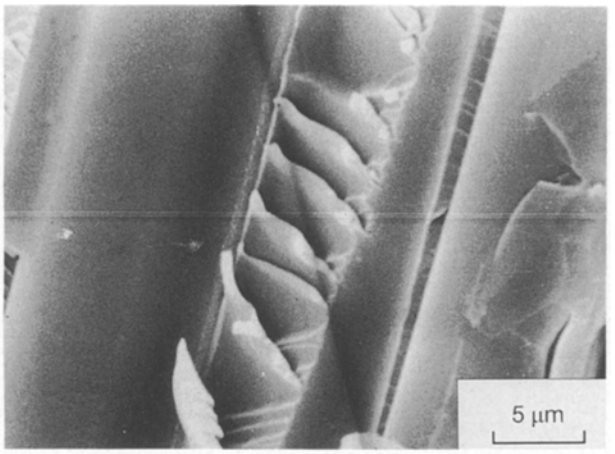

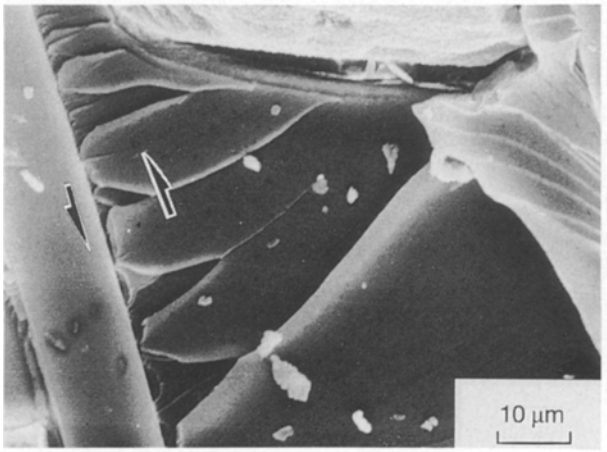

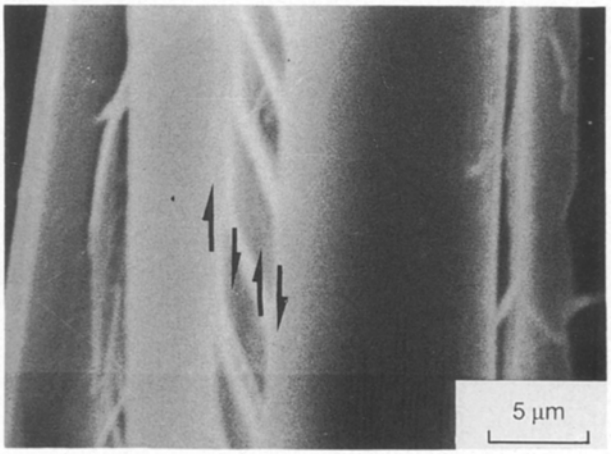

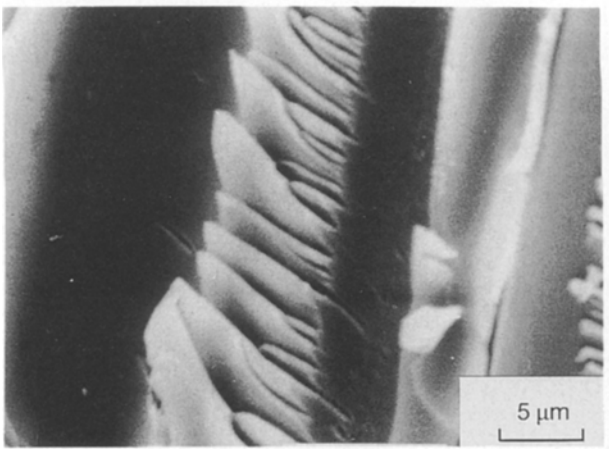

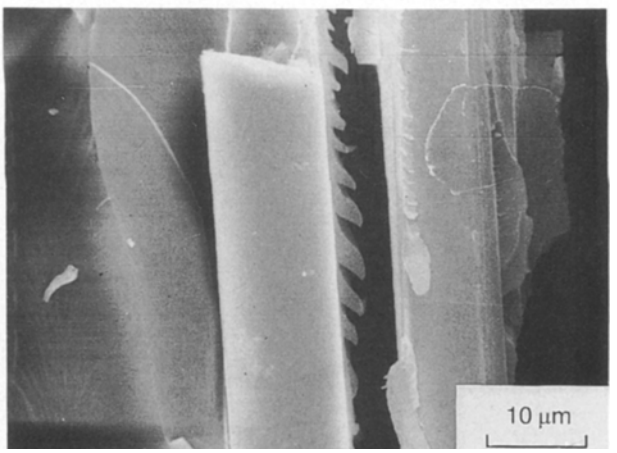

Figure 6 Sequential fibre–matrix interfacial failure in a resin-rich region: (a) microcracks formed at an angle to the fibre axis, (b) secondary cracks connecting the fibre to the primary cracks due to an unbalanced shear couple acting along the interface, (c) cusps formed at the interface due to separation of resin at the crack boundaries.

Figure 7 Sequential fibre–matrix interfacial failure in a fibre-rich region: (a) hackles and scallops between two adjacent fibres, (b) unbalanced shear deformation (marked by arrows), (c) formation of miniscule cusps due to hackle separation.

In resin-rich regions during shear loading as in the present case, the principal tensile stresses are oriented at an angle to the plane of applied shear as described by the Mohr circle. It is known that the matrix fracture occurs in a microscopic plane normal to the resolved tensile stress. As the loading or strain is increased, the microcracks that are formed ahead of the main crack-front branch into the interface, which results in curved platelets of resin. Here, as the shear is along the fibre–matrix interface, further separation causes the exposure of the curved platelets along the fibres. This is illustrated in Fig. 6a–c. In fibre-rich regions, due to the narrow region of resin between the fibres and the proximity to each other, of the shear couples along the two interfaces, the above phenomena occur in a different manner as discussed earlier.

The loading rate (at least in the present range) and the formulation of the resin seem to have a negligible effect on the fracture surface features and the failure

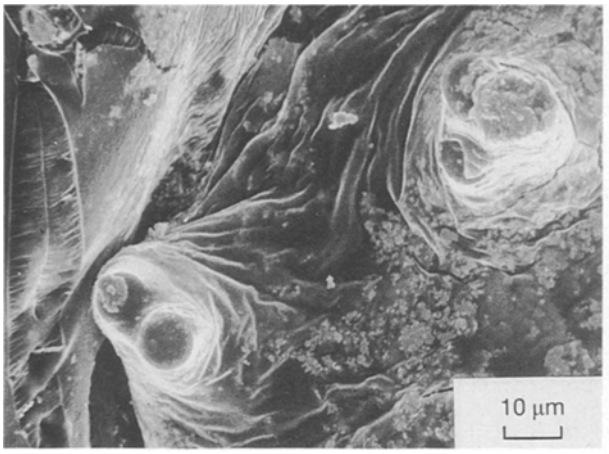

Figure 8 Resin microflow in a sample failed at a loading rate of 0.35 mm s^{-1}.

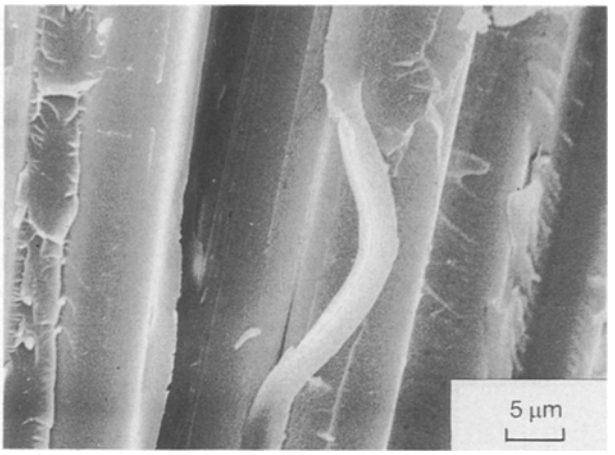

Figure 10 Buckling of resin along transverse fibres situated in the loading direction.

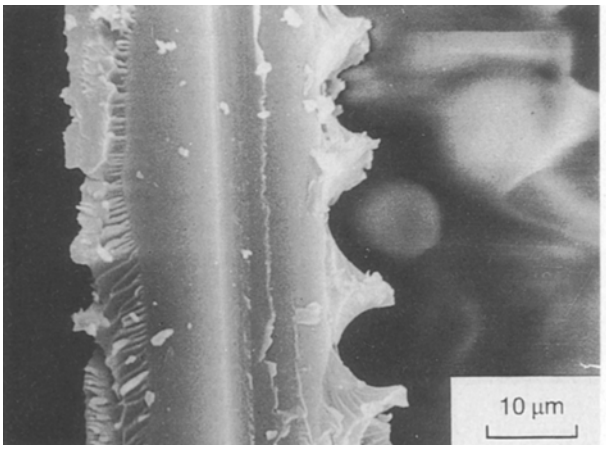

Figure 9 Peel-like failures in the tensile face of resin along the transverse fibres.

Figure 11 Chop marks on the fibres formed at an angle on the compression face of the sample.

sequences of the two composites considered. At the highest loading rate (0.35 mm s^{-1}) resin microflow was observed in the composite containing formulation I resin (Fig. 8).

Due to the debonding and pull-out of axial fibres in the tensile face, the resin along the transverse fibres shows peel-like failures as shown in Fig. 9.

On the compression side of the samples, resin buckling was observed along the loading direction as shown in Fig. 10. The chop marks [13] on the fibres, which are characteristic of compressive failures, seem to be inclined at an angle, due to the shear along the depth and the width of the sample being appreciable (Fig. 11).

4. Conclusions

The following conclusions may be drawn from the present study:

1. The isochronous modulus–strain plots reveal a greater non-linearity in the composite cured with resin formulation II. Further, the E_B values are also lower for this composite. This has been attributed to the increased degree of misalignment of the fibres, due to the presence of voids.

2. The MFS values show a marginal loading-rate sensitivity for both the composites. Crack-tip blunting, bowing-out and the presence of voids have been shown to produce a compensatory effect, thus explaining the observed trend.

3. Fracture mechanisms have been propounded for the translaminar fracture, based on the fibre–matrix interfacial shear couple concept. Fractographic observations in fibre-rich and resin-rich regions have been presented along with other salient features.

4. The loading rate and the formulation of the resin seem to have little effect on the observed fracture features.

Acknowledgements

The authors are grateful to Dr R. Vijayraghavan, Solid State Structural Chemistry Unit, and to the Chairman of the Department of Metallurgy, Indian Institute of Science, Bangalore for their help and interest shown during the various stages of this investigation.

References

1. C. ZWEBEN, W. S. SMITH and M. W. WARDLE, in "Composite Materials: Testing and Design (Fifth Conference) ",

ASTM STP 674, edited by S. W. Tsai (American Society for Testing and Materials, Philadelphia, 1979) p. 228.
2. P. K. MALLICK and L. J. BROUTMANN, *J. Testing Eval.* **5** (3) (1977) 190.
3. K. PADMANABHAN, S. SASHIDHARA and KISHORE, *Mater. Forum* **15** (4) (1991) 354.
4. B. GERSHON and G. MAROM, *J. Mater. Sci.* **10** (1975) 1549.
5. S. FISCHER, G. MAROM and F. R. TULER, *ibid.* **14** (1979) 863.
6. K. PADMANABHAN and KISHORE, *Bull. Mater. Sci.* **13**, (4) (1990) 245.
7. M. DAVIDOVITZ, A. MITTLEMAN, I. ROMAN and G. MAROM, *J. Mater. Sci.* **19** (1984) 377.
8. ASTM D790M - 84, "Flexural properties of unreinforced and reinforced plastics and electrical insulating materials (Metric) ", in Annual Book of ASTM Standards, Vol. 08.01 (American Society for Testing and Materials, Philadelphia, 1989).
9. C. B. BUCKNALL, "Toughened Plastics", (Applied Science, London, 1977) p. 108.
10. S. W. TSAI, "Structural behaviour of Composite Materials", NASA CR-71 (1964).
11. C. D. ELLIS and B. HARRIS, *J. Compos. Mater.* **7** (1973) 76.
12. S. M. LEE (ed.), "International Encyclopedia of Composites", Vol. 2 (VCH, New York, 1990) p. 268.
13. D. PURSLOW, *Composites* **12** (4) (1981) 241.

Received 10 April 1992
and accepted 25 January 1993